THE JOURNAL OF PHYSICAL CHEMISTRY A

Article

Cite This: J. Phys. Chem. A 2019, 123, 5081−5090

pubs.acs.org/JPCA

Physical Nature of Differential Spin-State Stabilization of Carbenes by Hydrogen and Halogen Bonding: A Domain-Based Pair Natural Orbital Coupled Cluster Study

Reza Ghafarian Shirazi,[†,‡] Frank Neese,*[,†] Dimitrios A. Pantazis,*[,†] and Giovanni Bistoni*[,†]

[†]Max-Planck-Institut für Kohlenforschung, Kaiser-Wilhelm-Platz 1, 45470 Mülheim an der Ruhr, Germany

[‡]Fakultät für Chemie und Biochemie, Ruhr-Universität Bochum, 44780 Bochum, Germany

Supporting Information

ABSTRACT: The variation in the singlet−triplet energy gap of diphenylcarbene (DPC) upon interaction with hydrogen (water and methanol) or halogen bond (XCF_3, X = Cl, Br, I) donors to form van der Waals (vdW) complexes is investigated in relation to the electrostatic and dispersion components of such intermolecular interactions. The domain-based local pair natural orbital coupled cluster method, DLPNO−CCSD(T), is used for calculating accurate single−triplet energy gaps and interaction energies for both spin states. The local energy decomposition scheme is used to provide an accurate quantification to the various interaction energy components at the DLPNO−CCSD(T) level. It is shown that the formation of vdW adducts stabilizes the singlet state of DPC, and in the case of water, methanol, and ICF_3, it reverses the ground state from triplet to singlet. Electrostatic interactions are significant in both spin states, but preferentially stabilize the singlet state. For methanol and $ClCF_3$, London dispersion forces have the opposite effect, stabilizing preferentially the triplet state. The quantification of the energetic components of the interactions through the local energy decomposition analysis correlates well with experimental findings and provides the basis for more elaborate treatments of microsolvation in carbenes.

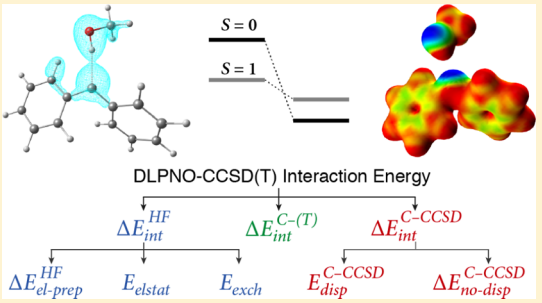

1. INTRODUCTION

Carbenes are highly reactive molecules that can typically be observed only in cryogenic situations or by means of ultrafast laser spectroscopy. Nevertheless, they were first proposed as intermediates of chemical transformations in 1855.[1] Since then, carbenes have been found to be crucial intermediates in a wide range of organic transformations;[2] they have been used as ligands in organometallic chemistry[3] and have recently been employed as organocatalysts.[4,5] Carbenes exist in either the singlet or the triplet state. As shown graphically in Figure 1, the central divalent carbon atom (i.e., the carbenic carbon C_{carb}) formally features a doubly occupied sp^2 and a vacant p orbital in the singlet state, whereas in the triplet state, both orbitals are singly occupied.

An important feature of the chemistry of carbenes is its spin specificity. In fact, singlet and triplet carbenes have different reactivity, with the former showing amphoteric behavior (i.e., they act as both Lewis acids and bases) and the latter acting as radicals. For instance, in the extensively studied reaction of alcohols with carbenes, triplet carbenes undergo insertion to C−H bonds, whereas singlet carbenes insert to O−H bonds.[6] The difference in reactivity of different spin states is explained by the Skell−Woodworth[7] rules, which describe how the reactions of singlet or triplet carbenes with singlet substrates differ because of the spin inversion requirement of the triplet state, leading to a stepwise reaction with a triplet biradical intermediate.

Because of the lone pair on the carbenic carbon, singlet carbenes can form a wide range of intermolecular complexes. Their unambiguous characterization is a very difficult task from an experimental point of view[8] and typically requires the synergy of experimental and computational studies. Examples of intermolecular carbene complexes are: (i) hydrogen-bonded or halogen-bonded complexes in which the carbene acts as electron donor;[9−11] (ii) weak O-ylidic complexes;[12−14] and (iii) weak charge-transfer π-complexes formed between aromatic donors and carbene acceptors.[13,15] In some cases, the interaction between the fragments is sufficiently strong for

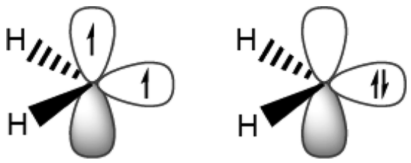

Figure 1. Schematic representation of the two low-lying spin states of CH_2: the triplet configuration $^3B_1$ (left) and the singlet configuration $^1A_1$ (right).

Received: February 1, 2019
Revised: March 21, 2019
Published: April 2, 2019

DOI: 10.1021/acs.jpca.9b01051
J. Phys. Chem. A 2019, 123, 5081−5090

the formed complexes to be considered as intermediates of chemical transformations.[16−18]

Importantly, these intermolecular interactions can modulate the lifetime, intersystem crossing, and reactivity rates of carbenes.[19−21] It has frequently been observed that polar solvents selectively stabilize the singlet state.[14,17] In the case of triplet ground-state carbenes, complexation with highly polar compounds can render the singlet state sufficiently accessible to participate in a reaction, or may even invert the singlet−triplet gap (E_{S-T}), resulting in a singlet ground state. For example, Costa and Sander recently showed that the formation of a hydrogen bond between diphenylcarbene (DPC) and methanol[10] or water[9] in argon matrix switches the ground state of DPC from triplet (hereafter denoted ^{3}DPC) to singlet (^{1}DPC). Further studies have shown that similar results are obtained for the interaction of DPC with halogen donors, such as ICF_3.[11] These results demonstrate that the relative hydrogen and halogen bond stabilization of ^{1}DPC compared to that of ^{3}DPC is larger than the E_{S-T} value, which is ca. 3 kcal/mol in vacuum.[22]

Although a wide range of computational studies have previously investigated the differential stabilization of the spin states of carbenes by means of implicit solvation models,[22−28] only a few took into account the role that direct intermolecular interactions play in this context.[22,27,29] In particular, Standard recently[27] applied correlated wavefunction-based methods to calculate E_{S-T} values of several carbenes as well as of their hydrogen-bonded complexes with water and methanol. It was found that in all cases hydrogen bonding selectively stabilizes the singlet state. Natural bond orbital analysis[30] showed that hydrogen bonding at the carbenic carbon is typically accompanied by a significant amount of charge transfer from the sp^2 lone pair to the antibonding σ^* O−H orbitals. The magnitude of charge transfer is significantly reduced in the triplet state, which qualitatively explains the observed differential spin-state stabilization. Halogen-bonding interactions with singlet carbenes have also been studied computationally in a number of studies,[29,31−36] but, to the best of our knowledge, a comparative study of the effect of such intermolecular interactions on the stabilization of singlet and triplet halogen-bonded complexes of carbenes has not been reported.

In either type of interaction, a wide range of different physical effects are expected to contribute to the stability of hydrogen- and halogen-bonded species, such as electrostatics, polarization, and London dispersion.[37] Hence, an in-depth, quantitative understanding of the physical mechanism responsible for the selective spin-state stabilization of carbenes by hydrogen and halogen bonding would require the simultaneous quantification of these energetic contributions for both singlet and triplet states. From a computational point of view, the use of density functional theory (DFT) for this purpose might be problematic because of the well-known difficulty of common functionals in accurately describing both the singlet−triplet energy gap and the weak interactions involved in the formation of these complexes.[22,27]

A recent benchmark study demonstrated that the canonical couple cluster theory CCSD(T) can be used for the accurate calculation of E_{S-T} values of aryl carbenes.[22] Although canonical CCSD(T) calculations are impractical for large carbenes, especially in cases of explicit complexation, approximations making use of the locality of electron correlation can be used to obtain reliable results for larger systems. In particular, the domain-based local pair natural orbital coupled cluster method with single, double, and perturbative triples excitations, DLPNO−CCSD(T),[38] was recommended as it provides accuracy comparable to that of canonical CCSD(T) at an affordable computational cost.[22] In addition to the attainment of highly accurate energetics for large systems, this approach provides an insightful way of analyzing intermolecular interactions in the framework of the so-called local energy decomposition (LED) analysis.[39,40] This approach allows one to decompose the binding energy of two (or more) molecules into repulsive electronic preparation, permanent and induced electrostatics, intermolecular exchange, and London dispersion. This scheme has been already applied in a wide range of contexts, including the study of hydrogen-bond interactions,[41] frustrated Lewis pairs,[42] and agostic interactions.[43]

In the present work, the DLPNO−CCSD(T)/LED methodology is used to elucidate the mechanism responsible for the selective spin-state stabilization upon complex formation for a series of hydrogen- and halogen-bonded complexes of DPC. Specifically, we investigate the interaction of DPC with methanol and water, as well as with a series of XCF_3 molecules (X = Cl, Br, I) (Figure 2). As the variation in the E_{S-T} values upon complexation depends on the difference between the binding energies in triplet and singlet states, the LED scheme can be used to quantify the most important interaction components in both states,[40] thus obtaining new physical insights into the differential stabilization of the singlet compared to the triplet.

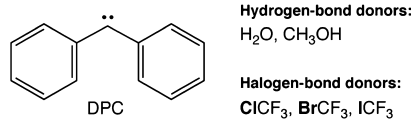

Figure 2. Compounds investigated in this study.

2. METHODOLOGY

2.1. Computational Details. All calculations were carried out using the ORCA software package version 4.1.[44] To select an optimal geometry optimization method, two density functionals and two wave function-based methods were compared for the systems DPC−CH_3OH, DPC−$ClCF_3$, and DPC−$BrCF_3$ in both singlet and triplet states. Geometry optimizations were carried out with B3LYP and B2PLYP in conjunction with dispersion corrections with the Becke−Johnson damping scheme[45,46] and with OO-MP2 and OO-SCS-MP2.[47] The def2-TZVPP basis sets[48] were used, and the resolution of identity (RI) approximation was applied in conjunction with appropriate RI basis sets.[49,50] Single-point DLPNO−CCSD(T) calculations were then performed at the optimized structures in order to identify which method produces geometries that are closest to the coupled cluster-level minimum. It was found that in most cases OO-SCS-MP2 provides structures with the lowest coupled cluster energy, and therefore, it was used for all geometry optimizations in the present work (Table S1). Structures were fully optimized in each state, using the "TightOPT" thresholds of ORCA.

Conformational searches were manually performed to identify possible alternative configurations. A low-energy minimum was identified for the singlet state for all adducts. For the triplet state, in addition to the expected conformation

DOI: 10.1021/acs.jpca.9b01051
J. Phys. Chem. A 2019, 123, 5081−5090

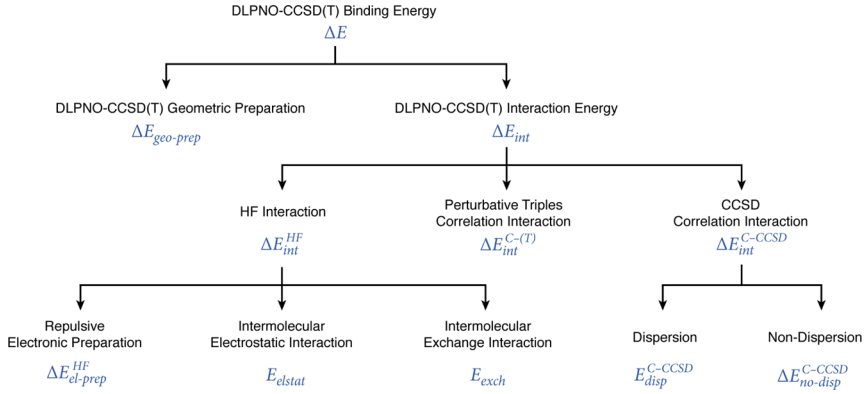

Figure 3. Energy terms in the DLPNO−CCSD(T)/LED framework.

featuring direct interaction with the carbene center, an alternative minimum for MeOH was identified, where the OH group interacts with the phenyl π-system. This type of structure (shown in Figure S1) is, however, energetically less favorable, and it will not be further considered in the present study. It is noted that for the case of MeOH we also explored possible interaction modes between DPC and two methanol molecules. As described in Figure S2 of the Supporting Information, for both singlet and triplet states, the possibility exists for simultaneous interaction of both MeOH molecules with the carbene center, but this is disfavored for both spin states. Instead, the second methanol molecule preferentially forms a hydrogen bond with the first methanol molecule that directly interacts with the carbene center, without significantly perturbing the nature of the DPC−MeOH interaction and the associated spin-state energetics.

Single-point DLPNO−CCSD(T) calculations were performed with "TightPNO" thresholds.[51,52] Quasi-restricted orbitals[53] (QROs) were used for the reference wave function. The extensively polarized valence quadruple-ζ def2-QZVPP[48] basis set was used in DLPNO−CCSD(T) calculations in conjunction with the corresponding RI basis set.[50] As shown in Tables S2 and S3, both the E_{S-T} gaps and the binding energies are converged with respect to the basis set. The contribution of the perturbative triples correction is included from a canonical CCSD(T) calculation with a smaller basis set as described previously.[22] Further information on the methodology is provided in the Supporting Information.

2.2. LED of Interaction Energies. The LED scheme has been extensively described in recent papers.[39,40,54] A short description is presented here. The DLPNO−CCSD(T) binding energy between two fragments X and Y can be written as

$$\Delta E = \Delta E_{\mathrm{geo-prep}} + \Delta E_{\mathrm{int}} \tag{1}$$

where the first term describes the geometric preparation energy (also called "strain") needed to distort the fragments X and Y from their equilibrium structure to the geometry they have in the complex. Hence, ΔE_{int} is the interaction energy between the distorted fragments. It can be further decomposed into a reference, $\Delta E_{\mathrm{int}}^{\mathrm{ref}}$, and a correlation contribution, $\Delta E_{\mathrm{int}}^{\mathrm{C}}$

$$\Delta E_{\mathrm{int}} = \Delta E_{\mathrm{int}}^{\mathrm{ref}} + \Delta E_{\mathrm{int}}^{\mathrm{C}} \tag{2}$$

Where $\Delta E_{\mathrm{int}}^{\mathrm{ref}}$ denotes the interaction energy computed at the reference level. In the closed shell case, the reference energy is the HF energy, and so $\Delta E_{\mathrm{int}}^{\mathrm{ref}}$ corresponds to the HF interaction energy. In the open shell case, the reference energy is the energy of a high-spin single determinant, which is constructed from a single set of molecular orbitals. In particular, QROs are used in the present study. These are extracted from the UHF procedure, as detailed in ref 53.

By exploiting the fact that occupied orbitals are localized in the DLPNO−CCSD(T) framework, $\Delta E_{\mathrm{int}}^{\mathrm{ref}}$ can be decomposed into electronic preparation and electrostatic and exchange interactions

$$\Delta E_{\mathrm{int}}^{\mathrm{ref}} = \Delta E_{\mathrm{el-prep}}^{\mathrm{ref}} + E_{\mathrm{elstat}} + E_{\mathrm{exch}} \tag{3}$$

where the electronic preparation, $\Delta E_{\mathrm{el\text{-}prep}}^{\mathrm{ref}}$, is always repulsive and corresponds to the energy required in order to distort the electron densities of the fragments from their ground state to the one that is optimal for the interaction. E_{elstat} and E_{exch} are the (permanent and induced) electrostatic and (attractive) exchange interactions, respectively, between the fragments.

The correlation contribution to the interaction energy, $\Delta E_{\mathrm{int}}^{\mathrm{C}}$, can be expressed as a sum of three contributions

$$\Delta E_{\mathrm{int}}^{\mathrm{C}} = \Delta E_{\mathrm{int}}^{\mathrm{C-SP}} + \Delta E_{\mathrm{int}}^{\mathrm{C-WP}} + \Delta E_{\mathrm{int}}^{\mathrm{C-(T)}} \tag{4}$$

in which $\Delta E_{\mathrm{int}}^{\mathrm{C\text{-}SP}}$, $\Delta E_{\mathrm{int}}^{\mathrm{C\text{-}WP}}$, and $\Delta E_{\mathrm{int}}^{\mathrm{C\text{-}(T)}}$ are the strong pairs, weak pairs, and triples correction components of the correlation contribution to the interaction energy, respectively. The sum of the $\Delta E_{\mathrm{int}}^{\mathrm{C\text{-}WP}}$ and $\Delta E_{\mathrm{int}}^{\mathrm{C\text{-}SP}}$ terms gives the DLPNO−CCSD correlation contribution to the interaction energy, which can be further divided into dispersive ($E_{\mathrm{disp}}^{\mathrm{C\text{-}CCSD}}$) and non-dispersive ($\Delta E_{\mathrm{no\text{-}disp}}^{\mathrm{C\text{-}CCSD}}$) correlation components, as already described previously.[54] Collecting all terms we obtain for the binding energy

$$\Delta E = \Delta E_{\mathrm{geo-prep}} + \Delta E_{\mathrm{el-prep}}^{\mathrm{ref}} + E_{\mathrm{elstat}} + E_{\mathrm{exch}} + E_{\mathrm{disp}}^{\mathrm{C-CCSD}} + \Delta E_{\mathrm{no-disp}}^{\mathrm{C-CCSD}} + \Delta E_{\mathrm{int}}^{\mathrm{C-(T)}} \tag{5}$$

which is the base for the analysis that is reported in the following sections. All the above-mentioned terms are shown graphically in Figure 3.

It is worth mentioning here that the energy terms shown in Figure 3 are extracted from the localized molecular orbitals of the adduct and as such already incorporate all polarization and charge transfer effects occurring upon bond formation. For instance, the E_{elstat} term incorporates permanent and induced electrostatic contributions, whereas $\Delta E_{\mathrm{el\text{-}prep}}^{\mathrm{ref}}$ accounts for the so-called Pauli repulsion as well as for polarization effects. We have recently suggested a possible strategy for disentangling

DOI: 10.1021/acs.jpca.9b01051
J. Phys. Chem. A 2019, 123, 5081−5090

these effects in the LED scheme, which is already available in ORCA for closed-shell molecular species.[54]

This scheme can be used to investigate the physical mechanism responsible for the variation observed in the E_{S-T} values of chemical species upon the formation of a non-covalent interaction, as shown in ref 40. In the present case, we shall use this scheme to analyze a series of DPC···Y adducts, where Y are the hydrogen or halogen bond donors investigated herein. The E_{S-T} value for the adduct is defined as

$$E_{S-T}(\mathrm{DPC}\cdots\mathrm{Y}) = E(^3\mathrm{DPC}\cdots\mathrm{Y}) - E(^1\mathrm{DPC}\cdots\mathrm{Y}) \quad (6)$$

For the free DPC, the same quantity reads

$$E_{S-T}(\mathrm{DPC}) = E(^3\mathrm{DPC}) - E(^1\mathrm{DPC}) \quad (7)$$

By subtracting eqs 6 and 7, the variation in the singlet-triplet gap of DPC upon interaction with Y can be obtained

$$\begin{aligned}\Delta E_{S-T} &= E_{S-T}(\mathrm{DPC}\cdots\mathrm{Y}) - E_{S-T}(\mathrm{DPC})\\ &= [E(^3\mathrm{DPC}\cdots\mathrm{Y}) - E(^3\mathrm{DPC})] - [E(^1\mathrm{DPC}\cdots\mathrm{Y}) - E(^1\mathrm{DPC})]\\ &= [E(^3\mathrm{DPC}\cdots\mathrm{Y}) - E(^3\mathrm{DPC}) - E(\mathrm{Y})]\\ &\quad - [E(^1\mathrm{DPC}\cdots\mathrm{Y}) - E(^1\mathrm{DPC}) - E(\mathrm{Y})]\\ &= \Delta E(^3\mathrm{DPC}\cdots\mathrm{Y}) - \Delta E(^1\mathrm{DPC}\cdots\mathrm{Y})\end{aligned} \quad (8)$$

Hence, ΔE_{S-T} equals the difference between the ^{3}DPC···Y and ^{1}DPC···Y binding energies. In the following, the LED scheme will be used to decompose the ΔE (^{3}DPC···Y) and ΔE (^{1}DPC···Y) values according to eq 5. Hence, from eqs 5 and 8, one obtains

$$\begin{aligned}\Delta E_{S-T} = {} & \Delta\Delta E_{geo-prep} + \Delta\Delta E^{ref}_{el-prep} + \Delta E_{elstat} + \Delta E_{exch}\\ & + \Delta E^{C-CCSD}_{disp} + \Delta\Delta E^{C-CCSD}_{no-disp} + \Delta\Delta E^{C-(T)}_{int}\end{aligned} \quad (9)$$

This will be used in the present work to obtain insights into the physical mechanism responsible for ΔE_{S-T} in different systems.

Finally, the so-called dispersion interaction density (DID) function[54] is used to provide a spatial analysis of the extent of the London dispersion in the various adducts studied in this work. The DID function $\Gamma(\mathbf{r})$ (where $\mathbf{r} = (x, y, z)$ is the radius vector) can be defined as

$$\Gamma(\mathbf{r}) = \frac{1}{2}\sum_{i\in X}\sum_{j\in Y}\varepsilon_{ij}^{(disp)}\left(\frac{1}{N_i}|\varphi_i(\mathbf{r})|^2 + \frac{1}{N_j}|\varphi_j(\mathbf{r})|^2\right) \quad (10)$$

where i and j label the occupied orbitals [$\varphi_i(\mathbf{r})$ and $\varphi_j(\mathbf{r})$] located on fragments "X" and "Y", respectively. N_i and N_j are the corresponding occupation numbers and $\varepsilon_{ij}^{(disp)}$ represents the sum of all dispersion-like excitations associated with the ij pair, as detailed in ref 54.

3. RESULTS AND DISCUSSION

3.1. Geometries of Adducts and Singlet−Triplet Gaps. The optimized geometries of all adducts are shown in Figure 4.

The computed E_{S-T} values for the systems shown in Figure 2 are reported in Table 1. In the same table, ΔE_{S-T} is the difference between the E_{S-T} of DPC complexes and that of the free DPC (eq 8). The S−T gaps calculated for the hydrogen-bonded complexes are consistent with the S−T gaps reported by Standard[27] using canonical coupled cluster theory. In Table S4 we have compared the S−T gaps for the DPC−H_2O complex calculated using several different methods. It is noted that in agreement with previous studies,[22,27] spin inversion is

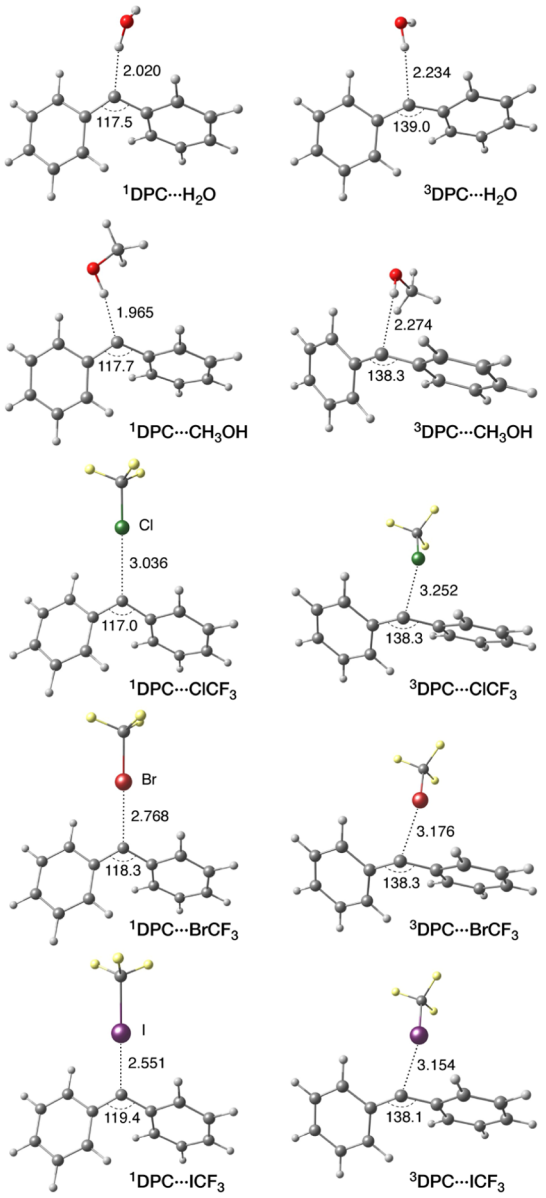

Figure 4. Optimized geometries of adducts discussed in this paper, with selected parameters (distances in Å, angles in degrees). Singlet states are shown on the left, triplet states on the right.

Table 1. Singlet Triplet Splitting (E_{S-T} in kcal mol^{-1}) of DPC and Its Complexes at the DLPNO−CCSD(T) Level of Theory[a]

system	E_{S-T}	ΔE_{S-T}
DPC	−3.34	0.00
DPC···H_2O	2.03	5.37
DPC···CH_3OH	1.57	4.91
DPC···CF_3Cl	−2.10	1.24
DPC···CF_3Br	−0.70	2.64
DPC···CF_3I	3.33	6.67

[a]Negative numbers indicate a triplet ground state. ΔE_{S-T} is the variation of E_{S-T} occurring upon bond formation, that is, E_{S-T} (complex)−E_{S-T} (DPC).

DOI: 10.1021/acs.jpca.9b01051
J. Phys. Chem. A 2019, 123, 5081−5090

Table 2. The Calculated Equilibrium ΔE Binding Energy (kcal/mol) of the Studied Molecular Adducts and Its Decomposition into the Reference (QRO) and DLPNO−CCSD(T) Correlation Energies Together with the Contribution Δ of Each Term to the Singlet−Triplet Gap

system	state	ΔE	$\Delta E_{\text{geo-prep}}$	ΔE_{int}	$\Delta E_{\text{int}}^{\text{ref}}$	$\Delta E_{\text{int}}^{\text{C}}$
DPC···H_2O	singlet	−8.79	0.53	−9.32	−5.79	−3.54
	triplet	−3.41	−0.48	−2.93	0.66	−3.59
	Δ	5.37	−1.02	6.39	6.45	−0.06
DPC···CH_3OH	singlet	−9.70	0.64	−10.35	−5.48	−4.87
	triplet	−4.80	0.13	−4.93	1.22	−6.14
	Δ	4.91	−0.52	5.42	6.69	−1.27
DPC···$ClCF_3$	singlet	−3.92	0.27	−4.19	−0.67	−3.52
	triplet	−2.68	0.06	−2.75	1.75	−4.50
	Δ	1.24	−0.21	1.44	2.42	−0.98
DPC···$BrCF_3$	singlet	−6.07	1.06	−7.13	−0.11	−7.02
	triplet	−3.43	0.10	−3.53	2.59	−6.13
	Δ	2.64	−0.96	3.59	2.70	0.90
DPC···ICF_3	singlet	−11.42	4.20	−15.62	−4.16	−11.46
	triplet	−4.75	0.14	−4.89	3.21	−8.10
	Δ	6.67	−4.06	10.73	7.37	3.36

not obtained for methanol and water when implicit solvation models are used.

The free DPC has a triplet ground state, with an E_{S-T} value of −3.3 kcal/mol at the DLPNO−CCSD(T) level. As shown in Table 1, adduct formation increases E_{S-T} in all cases ($\Delta E_{S-T} > 0$), consistent with previous studies. Hydrogen-bonded complexes show positive E_{S-T} values, meaning that they have a singlet ground state ($\Delta E_{S-T} \approx 5$ kcal/mol). In contrast, the E_{S-T} gap of halogen-bonded complexes increases with the size of the halogen atom. DPC−$ClCF_3$ and DPC−$BrCF_3$ maintain their triplet ground state and show only a small increase in their E_{S-T}, with ΔE_{S-T} being 1.2 and 2.6 kcal/mol, respectively. On the other hand, the DPC−CF_3I complex features the largest ΔE_{S-T} among the complexes studied in this work, 6.7 kcal/mol, thus featuring a singlet ground state.

The different nature of the interactions between the different molecules in the different spin states becomes apparent already by comparing the intermolecular distances between the DPC and the halogen/hydrogen-bonded donors of the complexes shown in Figure 4. All hydrogen-bonded complexes feature a short C_{carb}−HO contact and all halogen-bonded complexes a short C_{carb}−X (X = Cl, Br, I) contact, irrespective of the DPC spin state. Moreover, intermolecular distances decrease by increasing the size of halogen atom for both spin states. Hence, it appears that the hydrogen/halogen bond donors are involved in a rather directional interaction for both spin states of DPC. However, intermolecular distances are generally shorter in the singlet state, which is consistent with the fact that the intermolecular interactions preferentially stabilize the singlet state ($\Delta E_{S-T} > 0$). Although direct bond-length/bond-strength correlations are not generally valid in chemistry,[55] for the present series of adducts, this relation broadly holds based on the computed binding energies (Table S5).

All halogen-bonded complexes feature a C_{carb}−X−C angle close to 180° in the singlet state, whereas the same angle significantly deviates from linearity in the triplet state. In contrast, the C_{carb}−H−O angle is close to linearity for all hydrogen-bonded complexes. In the singlet state, the OH/C−X groups point directly toward the doubly occupied sp^2 orbital of ^{1}DPC in all complexes, whereas in the triplet state, they are typically oriented toward the singly occupied p orbital of ^{3}DPC. Accordingly, the C_{carb}−HO and C_{carb}−X bonds lie in the same plane defined by the two C_{carb}−C_{Ph} bonds in complexes of ^{1}DPC and are perpendicular to this plane in complexes of ^{3}DPC.

The only exception to this behavior is the ^{3}DPC···H_2O complex, in which the OH group points toward the singly occupied sp^2 orbital. A possible qualitative explanation of such geometrical differences is that both sp^2 and p orbitals are singly occupied in the triplet state, making the electron density distribution around the C_{carb} more isotropic than in the singlet state. Accordingly, there is no strictly favorable orientation for the hydrogen/halogen bond donor. Hence, it assumes the geometry that maximizes secondary interactions with the phenyl rings. Such secondary interactions are apparently negligible in H_2O, probably because of the small size of the molecule, which does not result in appreciable London dispersion attraction with the phenyl ring. The nature of these interactions will be discussed quantitatively in the next section by means of the LED scheme. It is worth stressing here that the above considerations are rigorously valid only for the formation of bimolecular adducts in the gas phase at low temperature and that the situation might be different in solution.

3.2. LED of Singlet and Triplet Adducts. Table 2 provides binding energies, ΔE, for the bimolecular carbene complexes shown in Figure 4 together with their decomposition into geometric preparation, $\Delta E_{\text{geo-prep}}$, and interaction energy, ΔE_{int}, and of the latter into reference, $\Delta E_{\text{int}}^{\text{ref}}$, and correlation, $\Delta E_{\text{int}}^{\text{C}}$, contributions. Furthermore, the contribution of each component of ΔE to the ΔE_{S-T} value is reported as the difference between the corresponding triplet- and singlet-state values, which is denoted as "Δ" in Table 2.

ΔE assumes a wide range of values for both singlet and triplet states. Although the ΔE_{S-T} values typically increase as the ΔE values increase, the trend does not correlate exactly with the binding energy in either the singlet or the triplet state. Hence, a quantitative understanding of the physical mechanism responsible for the variation in the E_{S-T} can be obtained only by analyzing the interaction in both states.

The hydrogen bond strengths (binding energies ΔE) are similar between water and methanol complexes. On the other hand, halogen bond strengths increase with the size of the halogen atom. The geometry preparation term $\Delta E_{\text{geo-prep}}$ is

DOI: 10.1021/acs.jpca.9b01051
J. Phys. Chem. A 2019, 123, 5081−5090

Table 3. LED of the Reference (QRO) and DLPNO−CCSD(T) Correlation Contributions to Interaction Energies (kcal/mol) for the Studied Molecular Adducts and the Contribution Δ of Each Term to the Singlet−Triplet Gap

		reference energy decomposition				correlation energy decomposition			
molecule	state	ΔE_{int}^{ref}	$\Delta E_{el\text{-}prep}^{ref}$	E_{elstat}	E_{exch}	$\Delta E_{int}^{C\text{-}CCSD(T)}$	$E_{Disp}^{C\text{-}CCSD}$	$\Delta E_{no\text{-}disp}^{C\text{-}CCSD}$	$\Delta E_{int}^{C\text{-}(T)}$
DPC···H_2O	singlet	−5.79	54.29	−51.16	−8.92	−3.54	−2.98	0.05	−0.60
	triplet	0.66	33.97	−25.29	−8.02	−3.59	−2.36	−0.55	−0.67
	Δ	6.45	−20.32	25.87	0.90	−0.06	0.61	−0.59	−0.07
DPC···CH_3OH	singlet	−5.48	62.80	−58.01	−10.27	−4.87	−4.02	0.01	−0.85
	triplet	1.22	33.79	−24.50	−8.07	−6.14	−4.72	−0.34	−1.08
	Δ	6.69	−29.02	33.51	2.20	−1.27	−0.69	−0.36	−0.22
DPC···$ClCF_3$	singlet	−0.67	36.09	−30.50	−6.27	−3.52	−3.15	0.31	−0.63
	triplet	1.75	18.24	−12.93	−3.57	−4.50	−3.54	−0.10	−0.78
	Δ	2.42	−17.85	17.57	2.70	−0.98	−0.40	−0.41	−0.15
DPC···$BrCF_3$	singlet	−0.11	125.64	−105.94	−19.81	−7.02	−5.73	0.03	−1.24
	triplet	2.59	37.23	−27.82	−6.83	−6.13	−4.52	−0.48	−1.01
	Δ	2.70	−88.41	78.12	12.99	0.90	1.21	−0.51	0.23
DPC···ICF_3	singlet	−4.16	291.54	−246.72	−48.98	−11.46	−10.52	1.20	−2.07
	triplet	3.21	54.43	−38.91	−12.31	−8.10	−5.99	−0.73	−1.29
	Δ	7.37	−237.10	207.80	36.67	3.36	4.53	−1.94	0.78

typically negligible, with the only exception being the ICF_3 complex in the singlet state. In this system, the C−I bond is significantly elongated with respect to the equilibrium geometry of ICF_3 and the C_{carb}−I distance is remarkably short. It is noted that in the study of Henkel et al.[11] on the interaction of DPC with ICF_3, a second type of adduct was suggested in addition to the classical halogen-bonded complex, that is, an ion pair structure in which the iodine atom is transferred to the carbenic carbon and interacts with CF_3^-. This non-classic complex was suggested to be slightly lower in energy, with a small conversion barrier, but the results were not conclusive.[11] Relaxed surface scans of the C_{carb}−I distance using various functionals are presented in Figure S3. Most methods predict only one minimum corresponding to the classic halogen-bonded structure, except PBE0 and B2PLYP, which also predict a second minimum at <2.1 Å associated with the ion pair structure. Thus, it is difficult from DFT calculations to decide on the nature of the PES. However, DLPNO−CCSD(T) calculations along the B2PLYP potential energy surface confirm that both minima exist and are close in energy (within ca. 1 kcal mol^{-1}), in agreement with the CASPT2 estimate of Henkel et al. For the purposes of the present study, we will further discuss only the classical halogen-bonding adduct.

Even though the formation of the ^{1}DPC···ICF_3 bond is accompanied by a significant $\Delta E_{geo\text{-}prep}$, binding energies ΔE typically follow the same trend as interaction energies ΔE_{int}. Hence, the ΔE_{int} contributions to ΔE_{S-T} correlate well with the overall ΔE_{S-T}. Having established this relationship, it is now instructive to decompose ΔE_{int} into reference, ΔE_{int}^{ref}, and correlation, ΔE_{int}^{C}, contributions.

ΔE_{int}^{ref} is attractive for singlet states and repulsive for triplet states, whereas ΔE_{int}^{C} is always negative and very large, especially for heavy (Br, I) halogen-bonded complexes. Hence, electron correlation is fundamental for the qualitative description of the interaction between the DPC and its bonding partner, especially for triplet states. Nevertheless, the ΔE_{int}^{ref} contribution to ΔE_{S-T} is typically larger than the corresponding ΔE_{int}^{C} contribution. As London dispersion is a correlation effect, these results suggest that London dispersion plays a fundamental role in determining the stability of intermolecular DPC complexes but has a relatively minor impact on ΔE_{S-T}. A more quantitative insight into the physical mechanism responsible for the trend of ΔE_{S-T} can be obtained by analyzing the LED terms reported in Table 3.

As mentioned above, in the LED scheme, ΔE_{int}^{ref} is decomposed into a repulsive component called electronic preparation, $\Delta E_{el\text{-}prep}^{ref}$, describing the perturbation of the electronic structures of the monomers upon the interaction and two intermolecular energy terms called electrostatic E_{elstat} and exchange E_{exch} interactions. Typically, the stronger the interaction is, the more the electron density of the binding partners is perturbed (polarization), leading to large and positive $\Delta E_{el\text{-}prep}^{ref}$ terms. This term also includes a repulsive energy component that can be associated with the so-called "Pauli Repulsion" commonly found in Morokuma-type energy-decomposing schemes. In stable adducts, these repulsive contributions are counteracted by the attractive (permanent and induced) electrostatic and exchange interactions, which are responsible for bringing the fragments together.

Consistent with the above considerations, the repulsive $\Delta E_{el\text{-}prep}^{ref}$ is much larger in the singlet state than in the triplet state. The attractive intermolecular exchange shows a similar trend but with opposite sign. In fact, the more the electron densities of the binding partners overlap, the stronger the attractive exchange interaction is.

E_{elstat} plays a major role in determining the overall sign of ΔE_{S-T} at the reference level, being always much larger in the singlet state than in the triplet state. Physically, the lone pair in the sp^2 orbital of singlet carbenes determines a very anisotropic electron density distribution around C_{carb}. As a consequence, the map of the electrostatic potential of ^{1}DPC (Figure 5) displays negative values in the region of the lone pair that match perfectly with the area of positive electrostatic potential on the halogen (the so-called σ hole) or on the hydrogen, leading to large E_{elstat} values.

For ^{3}DPC, the electrostatic potential around C_{carb} is much more isotropic and shifted to more positive values, leading to small E_{elstat} values. In fact, E_{elstat} is so small that it cannot counteract the repulsive components in $\Delta E_{el\text{-}prep}^{ref}$, leading to positive ΔE_{int}^{ref} for triplet states.

As the area of positive electrostatic potential around C_{carb} increases with the polarizability of the halogens (Figure 5), E_{elstat} also increases with the size of the halogen, determining

DOI: 10.1021/acs.jpca.9b01051
J. Phys. Chem. A 2019, 123, 5081−5090

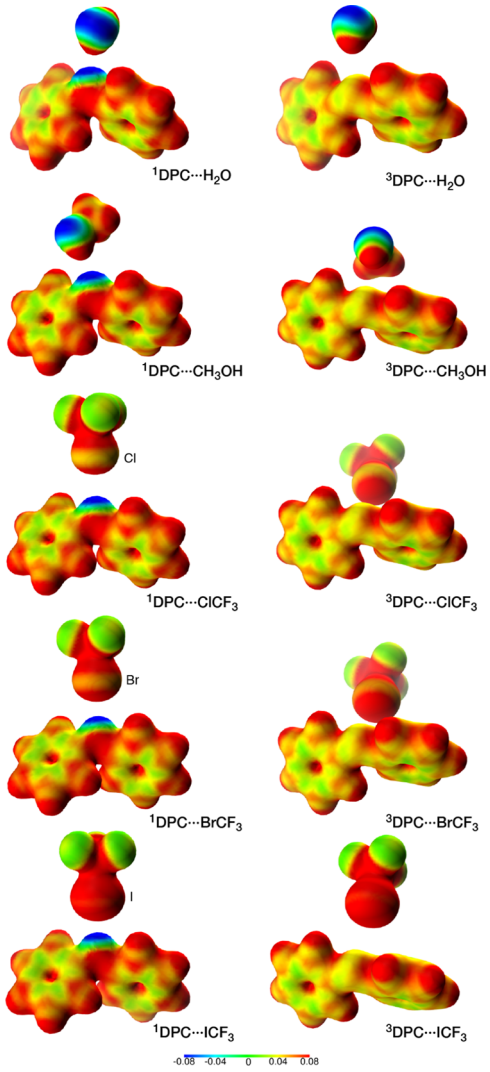

Figure 5. Electrostatic potential surfaces of the molecules included in this study calculated at the UHF level. The electrostatic potential (in a.u.) is mapped on electron density isosurfaces of 0.02 e/au^3. It was generated for the isolated fragments and superimposed in this figure in the relative orientation of the adduct structures.

the trend of the reference contribution to ΔE in the halogen-bonded complexes discussed above. In contrast, all hydrogen-bonded complexes show very similar electrostatic interactions for the same spin state.

In addition to the reference contribution, correlation significantly affects the binding energy of carbene complexes. In Table 3, the DLPNO−CCSD correlation energy is decomposed into dispersive $E_{disp}^{C\text{-}CCSD}$ and non-dispersive $\Delta E_{no\text{-}disp}^{C\text{-}CCSD}$ components. The contribution from the perturbative triples correction $\Delta E_{int}^{C\text{-}(T)}$ is also reported.

$\Delta E_{no\text{-}disp}^{C\text{-}CCSD}$ can be physically considered a correction to the reference energy terms.[54] Its contribution is relatively small for the complexes studied herein. Interestingly, it is positive for complexes in the singlet state and negative for complexes in the triplet state. It is worth mentioning here that $\Delta E_{no\text{-}disp}^{C\text{-}CCSD}$ incorporates a correction to the overestimated permanent electrostatics and to the underestimated induction energy at the reference level.[54] The first effect typically dominates when both the interacting species feature strong permanent multipoles, whereas the second effect becomes significant if only one of them has permanent multipoles.[54] Because of the different sign that $\Delta E_{no\text{-}disp}^{C\text{-}CCSD}$ assumes in singlet and triplet states, it contributes significantly to the overall ΔE_{S-T}.

The last significant physical contribution to the binding energy is the London dispersion term, $E_{disp}^{C\text{-}CCSD}$. It increases with the polarizabilities of the interacting partners and typically decays with the intermolecular distance R as R^{-6}.[37] Hence, we would expect $E_{disp}^{C\text{-}CCSD}$ to increase for larger atoms and shorter contact distances. However, even though singlet states feature shorter intermolecular distances, some complexes in the triplet state show secondary interactions with the phenyl rings. For methanol and $ClCF_3$, this leads to larger $E_{disp}^{C\text{-}CCSD}$ values in the triplet state. A further insight into this aspect can be obtained by looking at DID[54,56] plot shown in Figure 6. It shows a useful spatial analysis of the London dispersion component of the intermolecular interaction.

In the case of the hydrogen-bonded complexes, the main difference between water and methanol can be traced to the extra dispersion interaction provided by the methyl group,

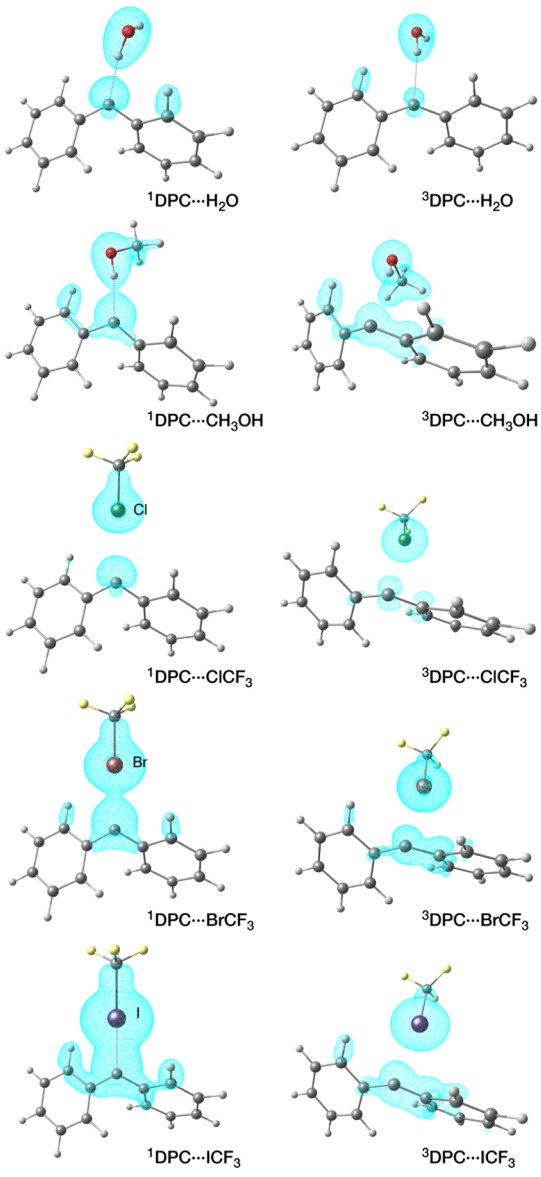

Figure 6. Dispersion plots of the different complexes included in this study. The plots are mapped at 0.0125 kcal/mol.

DOI: 10.1021/acs.jpca.9b01051
J. Phys. Chem. A 2019, 123, 5081−5090

which is a better dispersion energy donor (DED) than hydrogen.[57] For the DPC···methanol complex, $\Delta E_{disp}^{C\text{-}CCSD}$ is larger in the triplet state because of ability of the methyl group to interact with the phenyl ring, resulting in further dispersion. Hence, London dispersion stabilizes the triplet state more than the singlet state in the case of interaction of DPC with methanol, lowering the ΔE_{S-T} gap. The opposite is observed for the DPC−water complexes. Therefore, the presence of a DED group crucially affects the magnitude of the ΔE_{S-T} gap.

Among halogen-bonded complexes, dispersion increases from chlorine to iodine for both spin states. This agrees with chemical intuition, as the contact distance decreases and the polarizability of the halogen atom increases from chlorine to iodine. However, in chlorine, the shorter distance in the singlet state is compensated by the formation of secondary interactions with the phenyl ring in the triplet state, making the overall London dispersion contribution to the singlet−triplet gap slightly negative (i.e., it stabilizes preferentially the triplet state). This changes as the size of the halogen atom increases, with the C_{carb}−X contact dominating the overall dispersion contribution and hence rendering the latter the major factor in determining the differential spin-state stabilization ΔE_{S-T}.

4. CONCLUSIONS

In the present work, we investigated the energetic components that govern the interaction of DPC with hydrogen and halogen donors and the physics behind the differential stabilization of the singlet and triplet spin states upon adduct formation. Consistent with previous experimental and computational results, our DLPNO−CCSD(T) calculations predict that the singlet state is more strongly stabilized upon the formation of hydrogen or halogen bonds with respect to the triplet state. The stronger interaction in the case of the singlet state is sufficient to switch the ground state from the triplet of the isolated DPC to a singlet for the complexes with H_2O, CH_3OH, and ICF_3. The LED analysis was employed to decompose both the ^{1}DPC···X and the ^{3}DPC···X interaction energies in order to get insight into the physical mechanism responsible for the relative stabilization of the singlet state with respect to the triplet state.

For halogen-bonded adducts, the LED analysis demonstrates that electrostatic interactions significantly contribute to the DPC···X binding energy for both spin states of DPC. The stabilization of the singlet state can thus be understood in terms of the larger electrostatic interaction in ^{1}DPC···X than that in ^{3}DPC···X. In fact, ^{1}DPC has a lone pair that points directly toward the sigma hole. Consistent with this picture, the relative spin-state stabilization increases with the polarizability of the halogen atom, which in turn determines the size of the sigma hole. Also for hydrogen-bonded adducts, DPC···X electrostatic interactions play an important role for both spin states of DPC. The ^{1}DPC lone pair points directly toward the proton, and hence, even in this case, the electrostatic interaction is larger in ^{1}DPC···X than in ^{3}DPC···X.

London dispersion provides an additional contribution to the stability of DPC complexes for both spin states. In particular, intermolecular complexes of ^{3}DPC would not be stable without this fundamental component of the binding energy. In contrast to electrostatic interactions, London dispersion is only weakly affected by the spin state of DPC, and for methanol and $ClCF_3$, it stabilizes preferentially the triplet state.

Beyond the immediate relevance of the present results for understanding the physical nature of interactions involved in van der Waals complex formation between carbenes and hydrogen or halogen donors, the theoretical approach demonstrated in this work is entirely general. As such, this type of analysis is directly applicable to the investigation of weak interactions and of pre-reactive complexes for either closed- or open-shell systems. It is also expected that the insights into the physical origin of such interactions and the quantification of the distinct energetic contributions with the methods demonstrated in the present work can contribute to the development of new solvation models.

■ ASSOCIATED CONTENT

Supporting Information

The Supporting Information is available free of charge on the ACS Publications website at DOI: 10.1021/acs.jpca.9b01051.

Adducts of ^{3}DPC, models showing possible interaction modes of two methanol molecules, relaxed-surface scan, benchmarking of methods for geometry optimization of three different adducts, evaluation of the basis set effect, DLPNO−CCSD(T_0) interaction energies, S−T gaps, binding energies E and optimized C_{carb}−X bond lengths and Cartesian coordinates of all structures (PDF)

■ AUTHOR INFORMATION

Corresponding Authors

*E-mail: frank.neese@kofo.mpg.de (F.N.).
*E-mail: dimitrios.pantazis@kofo.mpg.de (D.A.P.).
*E-mail: giovanni.bistoni@kofo.mpg.de (G.B.).

ORCID

Frank Neese: 0000-0003-4691-0547
Dimitrios A. Pantazis: 0000-0002-2146-9065
Giovanni Bistoni: 0000-0003-4849-1323

Notes

The authors declare no competing financial interest.

■ ACKNOWLEDGMENTS

This work is supported by the Cluster of Excellence RESOLV (EXC 1069) funded by the Deutsche Forschungsgemeinschaft. Support by the Max Planck Society is gratefully acknowledged.

■ REFERENCES

(1) Hermann, M. Ueber die bei der technischen Gewinnung des Broms beobachtete flüchtige Bromverbindung. *Justus Liebigs Ann. Chem.* **1855**, *95*, 211−225.
(2) Chinoporos, E. Carbenes. Reactive Intermediates Containing Divalent Carbon. *Chem. Rev.* **1963**, *63*, 235−255.
(3) Schubert, U. Structural Consequences of Bonding in Transition Metal Carbene Complexes. *Coord. Chem. Rev.* **1984**, *55*, 261−286.
(4) Marion, N.; Díez-González, S.; Nolan, S. P. N-Heterocyclic Carbenes as Organocatalysts. *Angew. Chem., Int. Ed.* **2007**, *46*, 2988−3000.
(5) de Frémont, P.; Marion, N.; Nolan, S. P. Carbenes: Synthesis, Properties, and Organometallic Chemistry. *Coord. Chem. Rev.* **2009**, *253*, 862−892.
(6) Bethell, D.; Stevens, G.; Tickle, P. The reaction of diphenylmethylene with isopropyl alcohol and oxygen: the question of reversibility of singlet-triplet interconversion of carbenes. *J. Chem. Soc. D* **1970**, 792b−794.
(7) Woodworth, R. C.; Skell, P. S. Methylene, CH2. Stereospecific Reaction with cis- and trans-2-Butene. *J. Am. Chem. Soc.* **1959**, *81*, 3383−3386.

DOI: 10.1021/acs.jpca.9b01051
J. Phys. Chem. A 2019, 123, 5081−5090

(8) Arduengo, A. J. I.; Gamper, S. F.; Tamm, M.; Calabrese, J. C.; Davidson, F.; Craig, H. A. A Bis(Carbene)-Proton Complex: Structure of a C-H-C Hydrogen Bond. *J. Am. Chem. Soc.* **1995**, *117*, 572−573.
(9) Costa, P.; Fernandez-Oliva, M.; Sanchez-Garcia, E.; Sander, W. The Highly Reactive Benzhydryl Cation Isolated and Stabilized in Water Ice. *J. Am. Chem. Soc.* **2014**, *136*, 15625−15630.
(10) Costa, P.; Sander, W. Hydrogen bonding switches the spin state of diphenylcarbene from triplet to singlet. *Angew. Chem., Int. Ed.* **2014**, *53*, 5122−5125.
(11) Henkel, S.; Costa, P.; Klute, L.; Sokkar, P.; Fernandez-Oliva, M.; Thiel, W.; Sanchez-Garcia, E.; Sander, W. Switching the Spin State of Diphenylcarbene Via Halogen Bonding. *J. Am. Chem. Soc.* **2016**, *138*, 1689−1697.
(12) Moss, R. A.; Tian, J.; Sauers, R. R.; Krogh-Jespersen, K. Tracking ″Invisible″ Alkylchlorocarbenes by Their $\sigma \rightarrow$ p Absorptions: Dynamics and Solvent Interactions. *J. Am. Chem. Soc.* **2007**, *129*, 10019−10028.
(13) Moss, R. A.; Wang, L.; Weintraub, E.; Krogh-Jespersen, K. The Solvation of Carbenes: π andO-Ylidic Complexes ofp-Nitrophenylchlorocarbene. *J. Phys. Chem. A* **2008**, *112*, 4651−4659.
(14) Tomioka, H.; Ozaki, Y.; Izawa, Y. Modification of Singlet Carbene Reactivities by Solvent. *Tetrahedron* **1985**, *41*, 4987−4993.
(15) Moss, R. A.; Yan, S.; Krogh-Jespersen, K. Modulation of Carbenic Reactivity by π-Complexation to Aromatics. *J. Am. Chem. Soc.* **1998**, *120*, 1088−1089.
(16) Griller, D.; Nazran, A. S.; Scaiano, J. C. Reaction of Diphenylcarbene with Methanol. *J. Am. Chem. Soc.* **1984**, *106*, 198−202.
(17) Closs, G. L.; Rabinow, B. E. Kinetic Studies on Diarylcarbenes. *J. Am. Chem. Soc.* **1976**, *98*, 8190−8198.
(18) Eisenthal, K. B.; Turro, N. J.; Sitzmann, E. V.; Gould, I. R.; Hefferon, G.; Langan, J.; Cha, Y. Singlet-Triplet Interconversion of Diphenylmethylene. Energetics, Dynamics and Reactivities of Different Spin States. *Tetrahedron* **1985**, *41*, 1543−1554.
(19) Platz, M. S. A Perspective on Physical Organic Chemistry. *J. Org. Chem.* **2014**, *79*, 2341−2353.
(20) Tippmann, E. M.; Platz, M. S.; Svir, I. B.; Klymenko, O. V. Evidence for Specific Solvation of Two Halocarbene Amides. *J. Am. Chem. Soc.* **2004**, *126*, 5750−5762.
(21) Wang, J.; Kubicki, J.; Peng, H.; Platz, M. S. Influence of Solvent on Carbene Intersystem Crossing Rates. *J. Am. Chem. Soc.* **2008**, *130*, 6604−6609.
(22) Shirazi, R. G.; Neese, F.; Pantazis, D. A. Accurate Spin-State Energetics for Aryl Carbenes. *J. Chem. Theory Comput.* **2018**, *14*, 4733.
(23) Wang, Y.; Hadad, C. M.; Toscano, J. P. Solvent Dependence of the 2-Naphthyl(carbomethoxy)carbene Singlet−Triplet Energy Gap. *J. Am. Chem. Soc.* **2002**, *124*, 1761−1767.
(24) Wang, J.; Kubicki, J.; Hilinski, E. F.; Mecklenburg, S. L.; Gustafson, T. L.; Platz, M. S. Ultrafast Study of 9-Diazofluorene: Direct Observation of the First Two Singlet States of Fluorenylidene. *J. Am. Chem. Soc.* **2007**, *129*, 13683−13690.
(25) Cramer, C. J.; Truhlar, D. G.; Falvey, D. E. Singlet−Triplet Splittings and 1,2-Hydrogen Shift Barriers for Methylphenylborenide, Methylphenylcarbene, and Methylphenylnitrenium in the Gas Phase and Solution. What a Difference a Charge Makes. *J. Am. Chem. Soc.* **1997**, *119*, 12338−12342.
(26) Gonzalez, C.; Restrepo-Cossio, A.; Márquez, M.; Wiberg, K. B.; De Rosa, M. Ab Initio Study of the Solvent Effects on the Singlet−Triplet Gap of Nitrenium Ions and Carbenes. *J. Phys. Chem. A* **1998**, *102*, 2732−2738.
(27) Standard, J. M. Effects of Solvation and Hydrogen Bond Formation on Singlet and Triplet Alkyl or Aryl Carbenes. *J. Phys. Chem. A* **2017**, *121*, 381−393.
(28) Geise, C. M.; Wang, Y.; Mykhaylova, O.; Frink, B. T.; Toscano, J. P.; Hadad, C. M. Computational and Experimental Studies of the Effect of Substituents on the Singlet−Triplet Energy Gap in Phenyl(carbomethoxy)carbene. *J. Org. Chem.* **2002**, *67*, 3079−3088.
(29) Ge, Y.; Lu, Y.; Xu, Z.; Liu, H. Controlling the Spin State of Diphenylcarbene Via Halogen Bonding: A Theoretical Study. *Int. J. Quantum Chem.* **2018**, *118*, No. e25616.
(30) Weinhold, F.; Landis, C. R.; Glendening, E. D. What Is NBO Analysis and How Is It Useful? *Int. Rev. Phys. Chem.* **2016**, *35*, 399−440.
(31) Li, Q.; Wang, Y.; Liu, Z.; Li, W.; Cheng, J.; Gong, B.; Sun, J. An Unconventional Halogen Bond with Carbene as an Electron Donor: An Ab Initio Study. *Chem. Phys. Lett.* **2009**, *469*, 48−51.
(32) Esrafili, M. D.; Mohammadirad, N. Insights into the strength and nature of carbene···halogen bond interactions: a theoretical perspective. *J. Mol. Model.* **2013**, *19*, 2559−2566.
(33) Del Bene, J. E.; Alkorta, I.; Elguero, J. Hydrogen-Bonded Complexes with Carbenes as Electron-Pair Donors. *Chem. Phys. Lett.* **2017**, *675*, 46−50.
(34) Del Bene, J. E.; Alkorta, I.; Elguero, J. Halogen Bonding with Carbene Bases. *Chem. Phys. Lett.* **2017**, *685*, 338−343.
(35) Lv, H.; Zhuo, H.-Y.; Li, Q.-Z.; Yang, X.; Li, W.-Z.; Cheng, J.-B. Halogen Bonds with N-Heterocyclic Carbenes as Halogen Acceptors: A Partially Covalent Character. *Mol. Phys.* **2014**, *112*, 3024−3032.
(36) Donoso-Tauda, O.; Jaque, P.; Elguero, J.; Alkorta, I. Traditional and Ion-Pair Halogen-Bonded Complexes between Chlorine and Bromine Derivatives and a Nitrogen-Heterocyclic Carbene. *J. Phys. Chem. A* **2014**, *118*, 9552−9560.
(37) Stone, A. *The Theory of Intermolecular Forces*; OUP: Oxford, 2013.
(38) Saitow, M.; Becker, U.; Riplinger, C.; Valeev, E. F.; Neese, F. A New near-Linear Scaling, Efficient and Accurate, Open-Shell Domain-Based Local Pair Natural Orbital Coupled Cluster Singles and Doubles Theory. *J. Chem. Phys.* **2017**, *146*, 164105.
(39) Schneider, W. B.; Bistoni, G.; Sparta, M.; Saitow, M.; Riplinger, C.; Auer, A. A.; Neese, F. Decomposition of Intermolecular Interaction Energies within the Local Pair Natural Orbital Coupled Cluster Framework. *J. Chem. Theory Comput.* **2016**, *12*, 4778−4792.
(40) Altun, A.; Saitow, M.; Neese, F.; Bistoni, G. Local Energy Decomposition of Open-Shell Molecular Systems in the Domain-Based Local Pair Natural Orbital Coupled Cluster Framework. *J. Chem. Theory Comput.* **2019**, *15*, 1616.
(41) Altun, A.; Neese, F.; Bistoni, G. Local Energy Decomposition Analysis of Hydrogen-Bonded Dimers within a Domain-Based Pair Natural Orbital Coupled Cluster Study. *Beilstein J. Org. Chem.* **2018**, *14*, 919.
(42) Bistoni, G.; Auer, A. A.; Neese, F. Understanding the Role of Dispersion in Frustrated Lewis Pairs and Classical Lewis Adducts: A Domain-Based Local Pair Natural Orbital Coupled Cluster Study. *Chem.—Eur. J.* **2017**, *23*, 865−873.
(43) Lu, Q.; Neese, F.; Bistoni, G. Formation of Agostic Structures Driven by London Dispersion. *Angew. Chem., Int. Ed.* **2018**, *57*, 4760−4764.
(44) Neese, F. Software Update: The Orca Program System, Version 4.0. *WIREs Comput. Mol. Sci.* **2018**, *8*, No. e1327.
(45) Grimme, S.; Ehrlich, S.; Goerigk, L. Effect of the Damping Function in Dispersion Corrected Density Functional Theory. *J. Comput. Chem.* **2011**, *32*, 1456−1465.
(46) Grimme, S.; Antony, S.; Krieg, H. A consistent and accurate ab initio parametrization of density functional dispersion correction (DFT-D) for the 94 elements H-Pu. *J. Chem. Phys.* **2010**, *132*, 154104.
(47) Kossmann, S.; Neese, F. Correlated Ab Initio Spin Densities for Larger Molecules: Orbital-Optimized Spin-Component-Scaled MP2 Method. *J. Phys. Chem. A* **2010**, *114*, 11768−11781.
(48) Weigend, F.; Ahlrichs, R. Balanced Basis Sets of Split Valence, Triple Zeta Valence and Quadruple Zeta Valence Quality for H to Rn: Design and Assessment of Accuracy. *Phys. Chem. Chem. Phys.* **2005**, *7*, 3297−3305.
(49) Weigend, F. Accurate Coulomb-Fitting Basis Sets for H to Rn. *Phys. Chem. Chem. Phys.* **2006**, *8*, 1057−1065.

DOI: 10.1021/acs.jpca.9b01051
J. Phys. Chem. A 2019, 123, 5081−5090

(50) Hellweg, A.; Hättig, C.; Höfener, S.; Klopper, W. Optimized Accurate Auxiliary Basis Sets for RI-MP2 and RI-CC2 Calculations for the Atoms Rb to Rn. *Theor. Chem. Acc.* **2007**, *117*, 587−597.
(51) Liakos, D. G.; Sparta, M.; Kesharwani, M. K.; Martin, J. M. L.; Neese, F. Exploring the Accuracy Limits of Local Pair Natural Orbital Coupled-Cluster Theory. *J. Chem. Theory Comput.* **2015**, *11*, 1525−1539.
(52) Liakos, D. G.; Hansen, A.; Neese, F. Weak Molecular Interactions Studied with Parallel Implementations of the Local Pair Natural Orbital Coupled Pair and Coupled Cluster Methods. *J. Chem. Theory Comput.* **2010**, *7*, 76−87.
(53) Neese, F. Importance of Direct Spin−Spin Coupling and Spin-Flip Excitations for the Zero-Field Splittings of Transition Metal Complexes: A Case Study. *J. Am. Chem. Soc.* **2006**, *128*, 10213−10222.
(54) Altun, A.; Neese, F.; Bistoni, G. The Effect of Electron Correlation on Intermolecular Interactions: A Pair Natural Orbitals Coupled Cluster Based Local Energy Decomposition Study. *J. Chem. Theory Comput.* **2019**, *15*, 215.
(55) Kaupp, M.; Danovich, D.; Shaik, S. Chemistry Is About Energy and Its Changes: A Critique of Bond-Length/Bond-Strength Correlations. *Coord. Chem. Rev.* **2017**, *344*, 355−362.
(56) Wuttke, A.; Mata, R. A. Visualizing Dispersion Interactions through the Use of Local Orbital Spaces. *J. Comput. Chem.* **2017**, *38*, 15−23.
(57) Wagner, J. P.; Schreiner, P. R. London Dispersion in Molecular Chemistry—Reconsidering Steric Effects. *Angew. Chem., Int. Ed.* **2015**, *54*, 12274−12296.

DOI: 10.1021/acs.jpca.9b01051
J. Phys. Chem. A 2019, 123, 5081−5090